Boosting jet power in black hole spacetimes

David Neilsen[1,2], Luis Lehner[2,3,4], Carlos Palenzuela[5,6],
Eric W. Hirschmann[1], Steven L. Liebling[7], Patrick M. Motl[8], Travis Garrett[2,6]
[1] *Department of Physics and Astronomy, Brigham Young University, Provo, UT 84602, USA,*
[2] *Perimeter Institute for Theoretical Physics,Waterloo, Ontario N2L 2Y5, Canada,*
[3] *Department of Physics, University of Guelph, Guelph, Ontario N1G 2W1, Canada,*
[4] *CIFAR, Cosmology & Gravity Program, Canada,*
[5] *Canadian Institute for Theoretical Astrophysics, Toronto, Ontario M5S 3H8, Canada,*
[6] *Department of Physics & Astronomy, Louisiana State University, Baton Rouge, LA 70802, USA,*
[7] *Department of Physics, Long Island University, New York 11548, USA,*
[8] *Department of Science, Mathematics and Informatics,*
Indiana University Kokomo, Kokomo, IN 46904-9003, USA
(Dated: January 13, 2011)

The extraction of rotational energy from a spinning black hole via the Blandford-Znajek mechanism has long been understood as an important component in models to explain energetic jets from compact astrophysical sources. Here we show more generally that the kinetic energy of the black hole, both rotational and translational, can be tapped, thereby producing even more luminous jets powered by the interaction of the black hole with its surrounding plasma. We study the resulting Poynting jet that arises from single boosted black holes and binary black hole systems. In the latter case, we find that increasing the orbital angular momenta of the system and/or the spins of the individual black holes results in an enhanced Poynting flux.

I. INTRODUCTION

Enormously powerful events illuminate the universe that challenge our understanding of the cosmos. Indeed, intense electromagnetic emissions of order $\gtrsim 10^{51}$ergs [1–3] have been routinely observed in supernovae, gamma ray bursts (GRBs), and active galactic nuclei (AGNs), for example. However, despite important theoretical and observational advances, we still lack a thorough understanding of these systems (e.g. [4]). Intense observational and theoretical efforts are ongoing in order to unravel these fascinating phenomena. While the full details remain elusive, one of the natural ingredients in theoretical models is the inclusion of a rotating black hole which serves to convert binding and rotational energy of the system to electromagnetic radiation in a highly efficient manner. The starting point for these theoretical models can be traced back to ideas laid out by Penrose [5] and Blandford and Znajek (BZ) [6], which explain the extraction of energy from a rotating black hole. These seminal studies, along with subsequent work (see references in e.g. [7–9]), have provided a basic understanding of highly energetic emissions from single black hole systems interacting with their surroundings.

Recent work has indicated that related systems can also tap kinetic energy and lead to powerful jets [10]. This work concentrated on non-spinning black holes moving through a plasma and highlighted that relative black hole motion alone (with respect to a stationary electromagnetic field topology at far distances from it) can induce the production of jets. Furthermore, subsequent work [11] demonstrated that even black holes with misaligned spins with respect to the asymptotic magnetic field direction induce strong emissions with power comparable to the aligned case. These studies suggested that, independent of their inclination, astrophysical jets might be powered by the efficient extraction of both rotational and translational kinetic energy of black holes, and inducing even more powerful jets than the standard BZ mechanism would suggest.

Galactic mergers provide a likely scenario for the production of the binary black hole systems considered here [12, 13]. In such a merger, the supermassive black holes associated with each galaxy will ultimately form a binary in the merged galaxy. A variety of interactions will tighten the black hole binary. Eventually the dynamics of the system will be governed by gravitational radiation reaction which drives the binary to merge. The circumbinary disk will likely be magnetized and thereby anchor magnetic field lines, some of which will traverse the central region containing the binary. Preliminary observational evidence for supermassive black hole binaries resulting from galactic mergers has already been presented [14].

An ambient magnetic field threading a spinning black hole populates a low density plasma surrounding the black hole as explained by BZ [6]. Even for black holes with no spin, it was recently shown that the orbiting binary interacting with the surrounding plasma can lead to a collimated Poynting flux [10]. In this work, we consider this basic paradigm of energy extraction from black holes with the additional complexity of intrinsic black hole spin. Binaries consisting of spinning black holes demonstrate similar, albeit energetically enhanced, phenomenology. Furthermore, we investigate the dependence of the energy flux on the black hole velocity and highlight a resulting strong boost in the emitted power.

In addition to exquisite and powerful electromagnetic detectors, soon gravitational waves will be added to the arsenal of phenomena employed to understand our cos-

mos. These studies suggest excellent prospects for the coincident detection of both electromagnetic and gravitational signals from binary black hole systems. Certainly, dual detection of electromagnetic and gravitational wave signals would transform our understanding of these systems and lead to the refinement of theoretical models (e.g [15–18]).

In the remainder of this paper, we elucidate the basic phenomenology arising from the interaction of binary black hole systems immersed within a plasma environment. We focus in particular on understanding the Poynting flux emissions from such binaries as well as single, possibly spinning, black holes moving through plasma. We describe our equations and assumptions employed together with some of the details of our numerical implementation in Sec. II. Sec. III describes our results for both single and binary black holes and we provide concluding comments in Sec. IV.

II. IMPLEMENTATION DETAILS

The combined gravitational and electromagnetic systems that we consider consist of black hole spacetimes in which the black holes can be regarded as immersed in an external magnetic field. Such fields, as mentioned above, will be anchored to a disk. We consider this disk to be outside our computational domain but its influence is realized through the imposition of suitable boundary conditions on the corresponding electric and magnetic fields on the boundaries of our domain [10, 11]. With regard to the magnetosphere around the black holes, we assume that the energy density of the magnetic field dominates over its tenuous density such that the inertia of the plasma can be neglected. The magnetosphere is therefore treated within the force-free approximation [6, 19]. We note that the contribution of the energy density of the plasma to the dynamics of the spacetime is negligible and we can ignore its back reaction on the spacetime.

We use the BSSN formulation [20, 21] of the Einstein equations and the force-free equations as described in [10, 11]. We discretize the equations using finite difference techniques on a regular Cartesian grid and use adaptive mesh refinement (AMR) to ensure that sufficient resolution is available where required in an efficient manner. We use the HAD computational infrastructure, which provides distributed, Berger-Oliger style AMR [22, 23] with full sub-cycling in time, together with an improved treatment of artificial boundaries [24]. Refinement regions are determined using truncation error estimation provided by a shadow hierarchy [25], which adapts dynamically to ensure the estimated error is bounded by a pre-specified tolerance. Typically our adopted values result in a grid hierarchy yielding a resolution such that 40 grid points in each direction cover each black hole. We use a fourth order accurate spatial discretization and a third order accurate in time Runge-Kutta integration scheme [26]. We adopt a Courant parameter of $\lambda = 0.4$ so that $\Delta t_\ell = 0.4 \Delta x_\ell$ on each refinement level ℓ. In tests performed here for the coupled system (and in our previous works for the force-free Maxwell equations), the code demonstrates convergence while maintaining small constraint residuals for orbiting black holes. Furthermore, we obtain for orbiting black hole evolutions agreemend with runs from other codes for the same initial data.

To extract physical information, we monitor the Newman-Penrose electromagnetic (Φ_2) and gravitational (Ψ_4) radiative scalars [27]. These scalars are computed by contracting the Maxwell and the Weyl tensors respectively, with a suitably defined null tetrad (as discussed in [28]),

$$\Phi_2 = F_{ab} n^a \bar{m}^b \,, \quad \Psi_4 = C_{abcd} n^a \bar{m}^b n^c \bar{m}^d \,, \qquad (1)$$

and they allow us to account for the energy carried off by outgoing waves at infinity. The scalar Φ_2 (essentially the radial component of the Poynting vector) provides a measure of the electromagnetic radiation at large distances from an isolated system. However, as the system studied here has a ubiquitous magnetic field, special care must be taken to compute the energy flux. We account for this difficulty by subtracting the scalar $\Phi_0 = -F_{ab} l^a m^b$ from Φ_2. Hence, from here forward, by Φ_2 we mean the difference $\Phi_2 \to \Phi_2 - \Phi_0$. The luminosities in electromagnetic and gravitational waves are given by the integrals of the fluxes

$$L_{EM} = \frac{dE^{EM}}{dt} = \lim_{r\to\infty} \int r^2 |\Phi_2|^2 d\Omega \,, \qquad (2)$$

$$L_{GW} = \frac{dE^{GW}}{dt} = \lim_{r\to\infty} \int \frac{r^2}{16\pi} \left| \int_\infty^t \Psi_4 dt' \right|^2 d\Omega \,. \qquad (3)$$

We assume that the black holes are immersed in an initially constant magnetic field, such as one produced by a distant disk surrounding the black hole system. For the binary systems we consider, the orbital plane of the evolution is assumed to be aligned with that of the circumbinary disk. The magnetic field is anchored in the disk with its associated magnetic dipole aligned with the orbital angular momentum (chosen along the $\hat{z}$ direction). Initially, the magnetic field is set to be perpendicular to the velocity of the black holes and the electric field is set to zero. Because the electromagnetic field is affected by the spacetime curvature, it will be dynamically distorted from its initial configuration and generate a transient burst of both gravitational and electromagnetic waves as it settles into a physically relevant and dynamical configuration.

The initial magnitude of the magnetic field B_0 is chosen to be consistent with astrophysically relevant values [29, 30]. We present our results for a field strength which is bounded by the the Eddington magnetic field strength $B \simeq 6 \times 10^4 (M/10^8\, M_\odot)^{-1/2}$ G [31]. As noted above, for these values the plasma's energy is several orders of magnitude smaller than that of the gravitational field. Thus, although the plasma is profoundly affected by the black holes, it has a negligible influence on their dynamics.

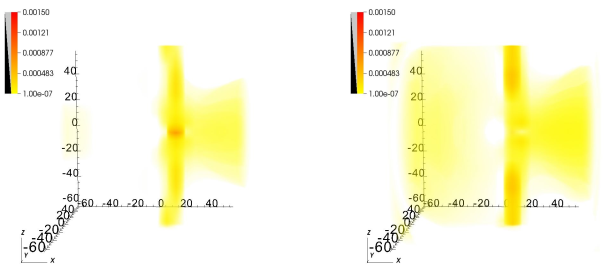

FIG. 1: Zoom-in of the electromagnetic emission $|r\Phi_2|^2$ from a boosted black hole (with $\vec{p} = 0.15\hat{x}$). The left frame shows the non-spinning black hole case ($a = 0$), while the right frame shows the spinning case ($a = 0.6$). The color scale is the same for both frames and the black hole is boosted to the right. The stronger emission in the vertically collimated region of the right frame is apparent.

III. RESULTS

Here we discuss our results for both boosted and binary black hole systems. For simplicity we introduce the notation $L_{43} = 10^{43}$ ergs/s and compute dimensionful quantities with respect to a representative system with total mass $10^8 M_\odot$ immersed in a magnetic field with strength 10^4 G. We explicitly provide proportionality factors for calculations for other configurations. Quantities in geometric units are calculated by setting $G = c = 1$.

Single black holes

For single, boosted black holes, we adopt a computational domain defined by $[-320\, m_b, 320\, m_b]^3$ and assume a fixed "bare" mass of the black hole (the mass it would have if it were static and in isolation) of $m_b = 1$ in geometric units. We set the initial linear momentum of the black hole to $\vec{p} = 0.05\, n\, \hat{i}$ (with n an integer that we vary between 0 and 4), and we set the intrinsic angular momentum parameter $\vec{a} \equiv \vec{J}/M^2$ to be 0 or $0.6\,\hat{k}$. For these parameters we study the resulting electromagnetic collimated flux energy and its dependence on both boost velocity and black hole spin.

Fig. 1 illustrates the qualitative features of the electromagnetic emission for a boosted black hole with and without spin. A collimated emission is clearly induced along the asymptotic magnetic field direction. Significantly, an even stronger emission is obtained for the spinning case as expected.

To achieve a more quantitative understanding, we compute a measure of the collimated electromagnetic luminosity, $L_{\rm collimated}$, by integrating the flux over a $15°$ cone of a spherical surface centered along the moving black hole with a radius $r = 20\, m_b$ (roughly equivalent to $40\, R_H$, where R_H is the Schwarzschild radius of the black hole). We present our results with respect to v (the measured *coordinate velocity* of the black hole) and plot the collimated luminosity achieved once the system reaches a quasi-stationary state (in other words, after the initial transient stage) for the spinning and non-spinning cases in Fig. 2.

Several key observations are evident from the figure. For $v = 0$, the electromagnetic energy luminosity does not vanish for the spinning black hole, while it does vanish for the non-spinning black hole. This is expected, as the spinning black hole interacts with a surrounding plasma and radiates by the Blandford-Znajek mechanism [6]. This luminosity results from the plasma's ability to extract rotational energy from the black hole and power a jet with an energy luminosity scaling as $L_{BZ} \approx \Omega_H^2 B^2$ [11, 32] (with $\Omega_H \equiv a/(2\, R_H)$ the rotation frequency associated with the black hole).

For $v \neq 0$, both the spinning and non-spinning black holes have a non-trivial associated energy flux. In the latter case this flux arises solely from the ability of the system to tap translational kinetic energy from the black hole, while the former results from the extraction of both translational and rotational kinetic energies.

The non-spinning black hole shows the expected v^2 dependence in the electromagnetic energy luminosity (see Fig. 2) consistent with the membrane picture of a black hole as a conductor. Indeed, as was already indicated in the spinless case [10, 11, 33, 34], a black hole moving (with speed v) through an ambient magnetic field acquires an induced charge separation ($\propto v$). The membrane paradigm [35] of a black hole explains this induced charge by regarding the black hole as a conductor moving through a magnetic field, and hence the induced charge is analogous to the classical Hall effect. With this observation and the induction equation, it is straightforward to conclude an electromagnetic energy flux will be produced with magnitude $\propto v^2 B^2$. Such a quadratic dependence on speed is apparent in the figure. These results are also consistent with the work of [36] which studied the Poynting flux associated with a moving conductor in a magnetized plasma, in particular the motion of artificial satellites in orbit. They found that this flux obeys $L_v \approx (v/v_{\rm alf})^2 B^2$ [36] where $v_{\rm alf}$, the propagation speed of the Alfvén modes, is the speed of light in a force-free environment. Furthermore, a misalignment is expected between the collimated energy flux and the original magnetic field orientation such that $\tan(\alpha) = v/v_{\rm alf}$. With the cautionary note that measuring this angle is a delicate enterprise within General Relativity, especially in the strongly curved region around the black hole, such a relation is manifested in our results. For instance, for $a = 0$, $p_x = 0.10$ the measured angle obeys $\tan(\alpha) = 0.07$ instead of the predicted 0.08 [36].

The luminosity for the spinning black hole also demonstrates the same quadratic dependence in velocity, with the additional component from the spin. Notice that the difference between the obtained luminosities in the spinning and spinless cases remains fairly constant for

the different values of v. Thus, to a reasonably good approximation, we can express the luminosity obtained as a sum of a spin dependent component and a speed dependent one, $L_{\rm collimated} \simeq L_{\rm spin} + L_{\rm speed}$, the latter scaling as $L_{\rm speed} = L_2 v^2$. A fit to the case $a = 0$ gives $L_2 = 127\ (M_8\, B_4)^2\, L_{43}$. Next, using this value for the case $a = 0.6$, we obtain the fit for $L_{\rm spin} = L_1 = 0.87\ (M_8\, B_4)^2\, L_{43}$. We can then provide an estimate of the associated luminosity for general cases as follows.

The spin component for the general case can be expressed in terms of its dependence on the the black hole spin as $L_{\rm spin} = L_1(\Omega_H(a)/\Omega_H(a=0.6))^2$. The boost component takes the already mentioned quadratic form $L_{\rm speed} = L_2 v^2$.

Therefore, we have for the estimate

$$\begin{aligned} L_{\rm collimated} &= L_{\rm spin} + L_{\rm speed}\,, \\ &= L_1 \left(\frac{\Omega_H|_a}{\Omega_H|_{0.6}}\right)^2 + L_2\, v^2\,, \\ &= \left[0.87 \left(\frac{\Omega_H|_a}{\Omega_H|_{0.6}}\right)^2 + 127 v^2\right] L_{43}. \end{aligned} \quad (4)$$

Notice that for $a = 0.6$, the non-rotational contribution $L_{\rm speed}$ to the emitted power becomes larger than the rotational one for speeds approximately $v > 0.08c$. This relationship, for example, would predict a luminosity for an $a = 0.95$, $v = 0.5c$ black hole to be $\simeq 36\, L_{43}(M_8\, B_4)^2$. This phenomenology strongly suggests that the Poynting flux can tap both rotational and translational kinetic energies from the black hole and that faster and more rapidly spinning black holes have a stronger associated power output.

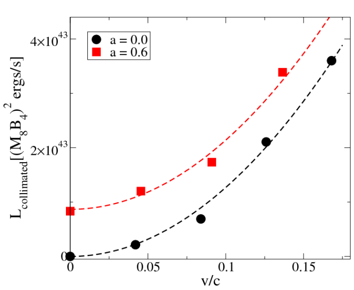

FIG. 2: Collimated luminosity as a function of the boost velocity of the black hole for two different spin magnitudes. The dashed lines are obtained from a quadratic fit of the form $L_{\rm collimated} = L_{\rm spin} + L_2 v^2$ where $L_{\rm spin}$ and L_2 are two constants. The constant L_2 is the same for both fits, supporting the argument that the luminosity does contain two different components, one for spin and one for boost.

Binary black holes

We turn our attention now to the orbiting binary black hole case. We consider equal-mass configurations in which each bare black hole has mass $m_b = 0.483$ and the pair is separated by a distance $D \approx 16\, m_b$. We adopt

Case	(p_x, p_y)	a_i	M_{ADM}	J_{ADM}
0/0	$(0.00208, -0.11235)$	0	1.0	0.108
u/d	$(0.00208, -0.11235)$	± 0.515	1.1	0.108
u/u	$(0.00208, -0.11235)$	0.515	1.1	0.349

TABLE I: Binary black hole configurations considered here. All begin with no momentum in the z direction.

a computational domain of $[-638\, m_b, 638\, m_b]^3$ and consider configurations with individual spins either vanishing or in the up ($+z$) or down ($-z$) orientation with spin magnitude $|a| = 0.515$. These configurations are summarized in Table I.

Before discussing these configurations, we describe our numerical measurements which enable a quantitative comparison between the evolutions. First, we compare the luminosities as functions of gravitational wave frequency, as this is an observable and allows for a direct comparison of the different cases. We obtain frequencies from the $l = 2, m = 2$ gravitational mode.

Second, we compute three different luminosities for each case: (i) the collimated luminosity $L_{\rm collimated}$ obtained by integrating the electromagnetic flux over a cone of points within 15° from the center of mass of the system; (ii) the non-collimated, or "isotropic," luminosity $L_{\rm isotropic}$ obtained from the integral over an encompassing sphere minus the collimated luminosity of (i); (iii) the gravitational wave luminosity, $L_{\rm GW}$. These different luminosities are displayed for the three binary configurations in Fig. 3.

Consider first the 0/0 and u/d configurations which have essentially the same total angular momentum. Extensive numerical simulations (see for instance [37]) and simple estimates [38] indicate that both binaries will merge into a final black hole with essentially the same spin ($a \simeq 0.67$), and, so for late times after-merger, the expected jet structure should be quite similar, dictated by the standard BZ mechanism.

The binary with individual spins aligned reaches a higher orbital velocity before merger than the previous two cases; thus, the expected maximum power should be higher. Moreover, the resulting final black hole spins faster ($a \simeq 0.8$) and thus its BZ associated power will be higher than that of the previous cases. Fig. 3 illustrates this expected behavior by presenting the Poynting flux energy vs. gravitational wave frequency for the three cases.

As evident from the figure, at low frequencies where the orbital dynamics are the same in all cases, both spinning cases have a higher output than the non-spinning one and the difference is provided by the spin contribution to the jet emission. Furthermore, both spinning cases have equal collimated power output because the spin contribution to the luminosity depends only on the spin magnitude.

We can further examine the basic relation explaining

the observed flux by comparing the three cases studied. We estimate the black hole *coordinate velocities* v and (collimated) luminosities at three representative frequencies $\Omega_i = \{1; 1.5; 2\}\, 10^{-5}$ [Hz/M_8] ($i = 1..3$) before the strong non-linear interaction starts. Since for these frequencies the measured speeds for the 0/0 and u/d cases are essentially the same, we notice that the flux of energy contributed by the spinning black holes can be estimated to be:

$$L^{est}_{BZ}(\Omega) \simeq L_{u/d}(\Omega) - L_{0/0}(\Omega)\,; \tag{5}$$

thus,

Ω	$(L_{0/0}; L_{u/d})(M_8 B_4)^2\, L_{43}$	$L^{est}_{BZ}(M_8 B_4)^2\, L_{43}$
1	(1.08; 1.62)	0.54
2	(1.83; 2.30)	0.47
3	(2.30; 2.80)	0.50

Notice that the L^{est}_{BZ} remains fairly constant through these frequencies which is evident also in the Fig. 3. With this value one can estimate the luminosity for the u/u case as:

$$L^{est}_{u/u}(\Omega) \simeq L_{0/0}(\Omega) \left(\frac{v_{u/u}(\Omega)}{v_{0/0}(\Omega)}\right)^2 + L^{est}_{BZ}(\Omega)\,. \tag{6}$$

Applying such expression to our representative values we obtain,

Ω	$(v_{u/u}; v_{0/0})$	$(L_{u/u}; L^{est}_{u/u})(M_8 B_4)^2\, L_{43}$
1	(0.192; 0.174)	(1.64; 1.85)
2	(0.206; 0.186)	(2.52; 2.71)
3	(0.211; 0.187)	(3.26; 3.42)

thus the estimates are within $\simeq$ 10% of the measured values while the black holes are sufficiently separated that their jets do not strongly interact. Notice that at higher frequencies the aligned (u/u) case indeed has a higher associated power.

In all cases, a significant non-collimated emission is induced (illustrated in the top right plot of Fig. 3) during the merger phase. Clearly, the simple minded picture of a jet produced by the superposition of the orbital and spinning effect can not fully capture the complete behavior at the merger epoch, although it serves to understand the main qualitative features and provides a means to estimate the power of the electromagnetic emission.

IV. FINAL COMMENTS

We have studied the impact of black hole motion through a plasma and indicated how the interaction can induce powerful electromagnetic emissions even for non-spinning black holes. Despite having examined a very small subset of the binary black hole parameter space, the results presented both here and in [10, 11] suggest a wide applicability to general black hole binaries. Moreover, as the plasma generally has a negligible effect on the dynamics of the black holes, then one needs only to know the dynamics of the black holes, say by numerical solution or other approximate methods, in order to estimate the expected electromagnetic luminosity. A recent example is the work of [39] which uses the expected $\simeq B^2 v^2$ scaling for non-spinning black hole binaries coupled with the known distance dependence in time to obtain excellent agreement with the obtained luminosity from such a system.

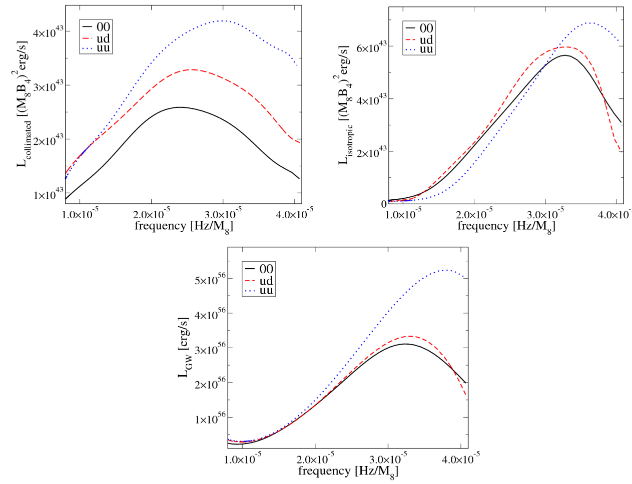

FIG. 3: Luminosity as a function of the orbital frequency for the binary black hole configurations described in Table I, assuming $M = 10^8 M_\odot$ and $B = 10^4$ G. **Top left:** the collimated luminosity associated with the jets. **Top right:** the isotropic luminosity representing electromagnetic flux not associated with the jets. **Bottom:** the gravitational wave output.

Naturally, spinning black holes produce stronger jets, and these jets, as shown earlier [11], will be aligned with the asymptotic magnetic field direction[42]. Thus, the resulting electromagnetic luminosity can be estimated to be $L^{EM}_{col} \simeq L_{\rm spin} + L_{\rm speed}$, which can be significant and have associated time-variabilities tied to the dynamical behavior of the system. In particular, the luminosity tied to the motion can result significantly higher than that tied to the spin. In addition, eccentric orbits and spin-orbit interactions driving orbital plane precessions can induce important variabilities that can aid in the detection of these systems. Furthermore, a significant pulse of nearly isotropic radiation is emitted during merger, thereby allowing observations of the system along directions not aligned with the jet.

Consequently, binary black hole interactions with surrounding plasmas can yield powerful electromagnetic outputs and allow for observing these systems through both gravitational and electromagnetic radiation. Gravitational waves from these systems corresponding to the last year before the merger could be observed to large

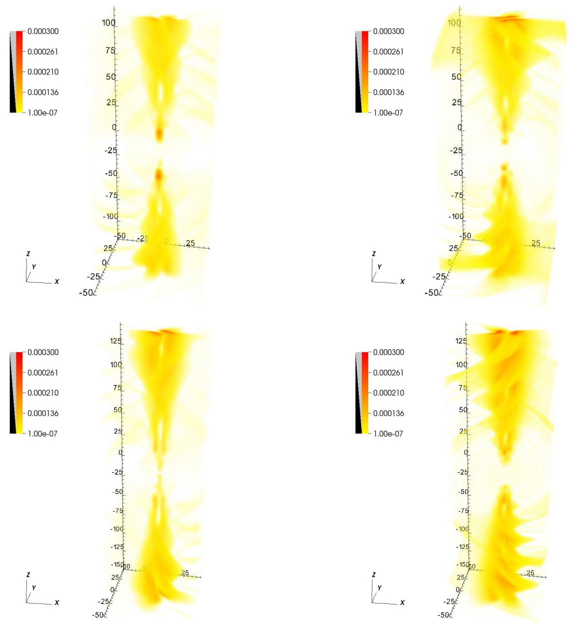

FIG. 4: Electromagnetic flux corresponding to the 0/0 (top row) and u/d (bottom row) cases at times $(-16.7, -2.5)$ hrs M_8 and $(-10.5, 3.6)$ hrs M_8 (with respect to the merger time as marked by the peak in strength of gravitational wave emission) respectively. The orbiting stage leaves its imprint as twisted tubes.

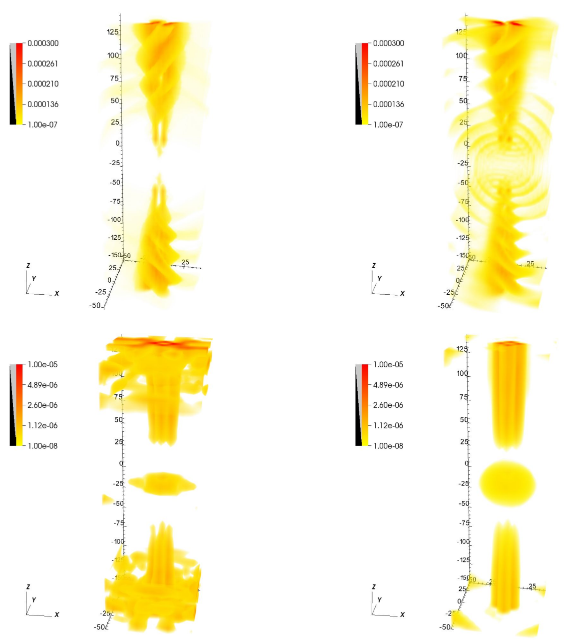

FIG. 5: Electromagnetic flux corresponding to the u/u case at times $(-2.5, 11.6, 40, 68)$ hrs M_8 (with respect to the merger time as marked by the peak in strength of gravitational wave emission). The orbiting behavior leaves a clear imprint in the resulting flux of energy and, as the merger proceeds emission along all directions is evident. At late times, the system settles to a single jet as dictated by the BZ mechanism.

distances with LISA (up to redshifts of 5-10 [40]) for masses $\simeq 10^{4-7} M_\odot$ or earlier in the orbiting phase (and possibly through merger) via Pulsar Timing Array observations [41], targeting binaries with masses in $M \simeq 10^{7-10} M_\odot$. As we have indicated here, both scenarios can have strong associated electromagnetic emissions. Our inferred luminosities of several $10^{43}(M_8 B_4)^2$ ergs/s corresponds to an isotropic bolometric flux of $F_x \simeq 10^{-15}$ erg $(M_8 B_4)^2$ /(cm^2 s) that could be detected to redshifts of $z \approx 1$ and even further depending on anisotropies, depending on the efficiency of processes taping this available energy and producing observable signals.

Acknowledgments

It is a pleasure to thank J. Aarons, P. Chang, B. MacNamara, K. Menou, E. Quataert and C. Thompson as well as our long time collaborators Matthew Anderson, Miguel Megevand and Oscar Reula for useful discussions and comments. We acknowledge support from NSF grants PHY-0803629 to Louisiana State University, PHY-0969811 to Brigham Young University, PHY-0969827 to Long Island University, as well as NSERC through a Discovery Grant. Research at Perimeter Institute is supported through Industry Canada and by the Province of Ontario through the Ministry of Research & Innovation. Computations were performed at LONI, Teragrid and Scinet.

[1] M. Hamuy (2003), astro-ph/0301006.
[2] S. E. Woosley and J. S. Bloom, Ann. Rev. Astron. Astrophys. **44**, 507 (2006), astro-ph/0609142.
[3] B. R. McNamara, M. W. Wise, P. E. J. Nulsen, L. P. David, C. L. Carilli, C. L. Sarazin, C. P. O'Dea, J. Houck, M. Donahue, S. Baum, et al., Ap. J. Letters **562**, L149 (2001), arXiv:astro-ph/0110554.
[4] R. Fender, E. Gallo, and D. Russell (2010), 1003.5516.
[5] R. Penrose, Riv. Nuovo Cim. **1**, 252 (1969).
[6] R. D. Blandford and R. L. Znajek, Mon. Not. Roy. Astron. Soc. **179**, 433 (1977).
[7] H. K. Lee, R. A. M. J. Wijers, and G. E. Brown, Physics Reports **325**, 83 (2000), arXiv:astro-ph/9906213.
[8] R. D. Blandford, in *Lighthouses of the Universe: The Most Luminous Celestial Objects and Their Use for Cosmology*, edited by M. Gilfanov, R. Sunyeav, & E. Churazov (2002), pp. 381–+.
[9] B. Punsly, ed., *Black Hole Gravitohydromagnetics*, vol. 355 of *Astrophysics and Space Science Library* (2008).
[10] C. Palenzuela, L. Lehner, and S. L. Liebling, Science **329**, 927 (2010), 1005.1067.
[11] C. Palenzuela, T. Garrett, L. Lehner, and S. L. Liebling, Phys. Rev. **D82**, 044045 (2010), 1007.1198.
[12] M. C. Begelman, R. D. Blandford, and M. J. Rees, Nature (London) **287**, 307 (1980).
[13] M. Milosavljevic and E. S. Phinney, Astrophys. J. **622**, L93 (2005).
[14] J. M. Comerford et al., Astrophys. J. **698**, 956 (2009), 0810.3235.
[15] B. F. Schutz, in *Lighthouses of the Universe: The Most Luminous Celestial Objects and Their Use for Cosmology*, edited by M. Gilfanov, R. Sunyeav, & E. Churazov (2002), pp. 207–+.
[16] J. Sylvestre, Astrophys. J. **591**, 1152 (2003), arXiv:astro-ph/0303512.
[17] J. S. Bloom, D. E. Holz, S. A. Hughes, K. Menou, A. Adams, S. F. Anderson, A. Becker, G. C. Bower, N. Brandt, B. Cobb, et al., ArXiv e-prints (2009), 0902.1527.
[18] E. S. Phinney, in *astro2010: The Astronomy and Astrophysics Decadal Survey* (2009), vol. 2010 of *Astronomy*, pp. 235–+.
[19] P. Goldreich and W. H. Julian, Astrophys. J. **157**, 869 (1969).
[20] T. W. Baumgarte and S. L. Shapiro, Phys. Rev. **D59**, 024007 (1999), gr-qc/9810065.
[21] M. Shibata and T. Nakamura, Phys. Rev. **D52**, 5428 (1995).
[22] Http://www.had.liu.edu/.
[23] S. L. Liebling, Phys. Rev. **D66**, 041703 (2002).
[24] L. Lehner, S. L. Liebling, and O. Reula, Class. Quant. Grav. **23**, S421 (2006).
[25] F. Pretorius, Ph.D. thesis, The University of British Columbia (2002).
[26] M. Anderson et al., Phys. Rev. **D77**, 024006 (2008).
[27] E. Newman and R. Penrose, J. Math. Phys. **3**, 566 (1962).
[28] L. Lehner and O. M. Moreschi, Phys. Rev. **D76**, 124040 (2007), 0706.1319.
[29] M. Massi and M. Kaufman, Astronomy and Astrophysics **477**, 1 (2008).
[30] G. B. Field and R. D. Rogers, Astrophys. J. **403**, 94 (1993).
[31] C. D. Dermer, J. D. Finke, and G. Menon, ArXiv e-prints (2008), 0810.1055.
[32] A. Tchekhovskoy, R. Narayan, and J. C. McKinney, Astrophys. J. **711**, 50 (2010), 0911.2228.
[33] C. Palenzuela, M. Anderson, L. Lehner, S. L. Liebling, and D. Neilsen, Phys. Rev. Lett. **103**, 081101 (2009), 0905.1121.
[34] C. Palenzuela, L. Lehner, and S. Yoshida, Phys. Rev. **D81**, 084007 (2010), 0911.3889.
[35] K. S. Thorne, R. H. Price, and D. A. MacDonald, *Black holes: The membrane paradigm* (1986).
[36] S. D. Drell, H. M. Foley, and M. A. Ruderman, Journal of Geophysical Research **70**, 3131 (1965).
[37] M. Hannam et al., Phys. Rev. **D79**, 084025 (2009), 0901.2437.
[38] A. Buonanno, L. E. Kidder, and L. Lehner, Phys. Rev. **D77**, 026004 (2008).
[39] S. T. McWilliams (2010), 1012.2872.
[40] A. Vecchio, Phys. Rev. **D70**, 042001 (2004), astro-ph/0304051.
[41] P. Demorest, J. Lazio, A. Lommen, and NANOGRAV collaboration (2009), 0902.2968.
[42] The magnitude of the BZ-associated emission diminishes for non-aligned cases but it is nevertheless significant: the orthogonal case is only half as powerful as the aligned case.